Planar Delamination Growth Of Composite Laminates Under Mode II Fatigue Loading

Tu, W.; Riberaygua, P. S.; Pascoe, J.A.; Alderliesten, R.C.

Important note
To cite this publication, please use the final published version (if applicable).
Please check the document version above.

ECCM21
02-05 July 2024
Nantes - France

Proceedings of the 21st European Conference on Composite Materials
Volume 8 - Special Sessions

648
1420

CONTENTS

PLANAR DELAMINATION GROWTH OF COMPOSITE LAMINATES UNDER MODE II FATIGUE LOADING

W. Tu[1*], P.S. Riberaygua[1], J.A. Pascoe[1] and R.C. Alderliesten[1]

[1]Department of Aerospace Structures and Materials, Faculty of Aerospace Engineering,
Delft University of Technology, Kluyverweg 1, 2629HS, Delft, The Netherlands
Email: W.Tu@tudelft.nl

Keywords: Fatigue, Polymer-matrix composites (PMCs), Planar delamination, Mode II

Abstract
For the past few decades, research into fatigue delamination behaviour of Carbon Fibre Reinforced Polymer (CFRP) composites has predominantly relied on standard test methods. These methods typically utilize a uniaxial delamination length to quantify the fatigue delamination process. However, this approach is inadequate to describe the nature of delamination growth in a planar manner. In this work, an experimental study was conducted to gain insights into the planar delamination behaviour of CFRP composites under mode II fatigue loading. Delamination growth of two specimen configurations, each containing an embedded initial defect, was monitored through ultrasound scanning (C-scan). During load-control fatigue testing, the growth rate exhibited an initial rise, followed by a subsequent decrease as loading cycles increased. Despite the development of a larger delamination area under fatigue loading, a consistent overall stiffness was observed. Fractography revealed the presence of various fracture mechanisms ocurring at different locations near the initial delamination front. Micro matrix cracking and fibre-matrix debonding emerged as dominant mechanisms in 2D fatigue delamination growth following the fibre direction. Matrix cracking within the laminate ply occurred at the locations where the growth direction deviated from the fibre direction, consequently triggering delamination migration.

1. Introduction

Over the past few decades, the fatigue behaviour of composite material has received substantial attention in aerospace structures or large wind turbines. Fatigue delamination is one of the most common damage modes in composite laminates, jeopardizing structural integrity. The ability to predict fatigue delamination growth is critical for the development of structural design and maintenance management. Predictive models for one-dimensional (1-D) fatigue delamination growth have been established, relying on standardized test methods such as Double Cantilever Beam (DCB) [1] and End Notched Flexure (ENF) [2]. Most of these models utilize a Paris-type equation [3] that correlates crack propagation rate $\mathrm{d}a/\mathrm{d}N$ with various fracture parameters, such as Stress Intensity Factor (SIF, K) or Energy Release Rate (ERR, G [4]), through experimental fitting [5]–[7], as indicated in the following equation:

$$\frac{\mathrm{d}a}{\mathrm{d}N} = C f(K, G)^n \tag{1}$$

where C and n are fitting coefficients and are highly dependent on material properties [8], [9], loading conditions [7], [10], [11], and specimen geometry [12]–[14].

ECCM21
02-05 July 2024
Nantes - France

Proceedings of the 21st European Conference on Composite Materials
Volume 8 - Special Sessions

649
1420

Difficulties arise when employing these models to predict fatigue delamination growth in actual structures, where two-dimensional (2D) planar delamination growth predominates as the principal damage pattern [14]–[16]. On the one hand, the measurement of growth rate based on uniaxial crack length is insufficient to describe multidirectional delamination growth. On the other hand, the determination of the stress or energy state at the delamination front for obtaining the fracture parameters is challenging.

A physical Energy Release Rate (ERR) method has demonstrated its ability to provide physics-based interpretation on the correlation between the fatigue delamination growth rate $\mathrm{d}A/\mathrm{d}N$ and energy dissipation rate $\mathrm{d}U/\mathrm{d}N$ [17]–[20]. This method was implemented on investigation of planar delamination growth under mixed-mode fatigue loading [21]. However, characterizing the physical ERR was challenging due to the influence of geometric nonlinearity and limitations in accurately measuring delamination growth.

2D mode I fatigue debonding in sandwich panels was investigated experimentally by Cameselle-Molares et al [14]. The experiment demonstrated a decreasing crack growth rate alongside an increasing cyclic energy dissipation under load control. This was in contrast with the results obtained from DCB fatigue tests under load control. Following which, planar delamination behaviour of GFRP composites under quasi-static mode II loading was investigated experimentally and numerically [22], [23]. Compared to End-Loaded Split (ELS) test results, a longer fracture process zone was discovered in planar delamination growth due to in-plane stretching. To the present authors' knowledge, there is still a lack of research regarding the planar delamination behaviour under mode II fatigue loading.

Therefore, an experimental method is developed in this study, aiming to investigate the planar delamination behaviour of CFRP composite lamintes under mode II fatigue loading. Delamination growth rate was measured through ultrasonic scanning (C-scan). The stiffness variation throughout the fatigue testing was analyzed based on cyclic loading curves. Furthermore, fractographic analysis using Scanning Electron Microscope (SEM) has revealed the planar delamination mechanisms of CFRP laminites under mode II fatigue loading.

2. Experiment

2.1. Material and specimen configurations

The material used in the experimental campaign is a unidirectional (UD) prepreg with DT120 epoxy thermosetting resin and carbon fibre reinforcement. The mechanical properties of the material are provided by a technical data sheet [24]. Two quasi-isotropic layups were designed to investigate the effect of interface angle and stacking sequence on planar delamination pattern. The specimen details are listed in Table 1. Delamination growth in the initial interface, where the artificial defect was embedded, tended to migrate to an adjacent interface. This migration occurred at the locations where the normal of the circular front was perpendicular to the fibre direction [16]. The interface where the migrated delamination propagates was indicated as the 'migration interface' in Table 1.

Table 1. Specimen details of planar delamination tests.

Specimen Type	Initial Interface	Migration Interface	Layup
PCLS(0//0)	0º//0º	0º//90º	$[0/90/45/-45]_s//^*[0/90/45/-45]_s$
PCLS(0//90)	0º//90º	90º//0º	$[0/90/45/-45]_s//[90/0/45/-45]_s$

* // indicates the interface where the initial delamination was embedded

As illustrated in Figure 1, a semi-complex specimen configuration, named Planar Central Loaded Split (PCLS), was designed for conducting planar delamination tests under mode II fatigue loading. An initial circular delamination, with a radius of 9 mm, was introduced at the middle interface by inserting a single

ECCM21
02-05 July 2024
Nantes - France

Proceedings of the 21st European Conference on Composite Materials
Volume 8 - Special Sessions

650
1420

CONTENTS

layer of Teflon sheet. The CFRP composite panels measured 140×140 mm^2, excluding the clamping region, and had a thickness of $2h = 2.5$ mm.
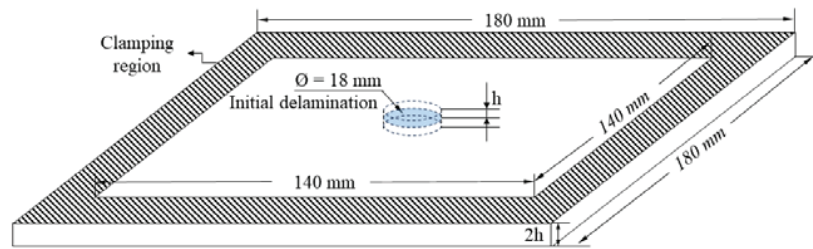
Figure 1. Illustration of PCLS specimen configuration.

2.2. Test setup

The experiment setup is illustrated in Figure 2. The machine used for the fatigue tests was an MTS 810 test frame with a 15kN load cell. An in-house designed test fixture was used to clamp the specimen, enabling the implementation of 3D Digital Image Correlation (DIC) analysis for obtaining surface strain variation throughout the test process. The specimen was fully clamped in the fixtures, and the slippage at the clamping region was prevented by inserting a rubber mat between the contact surfaces. To alleviate the stress concentration at the loading region, a circular rubber mat with a radius of 6 mm was attached to the indenter head, ensuring a more uniformly distributed loading at the lower surface of the specimen. In addition, acoustic emission sensors were attached to the specimens in order to detect damage initiation in the fatigue test.
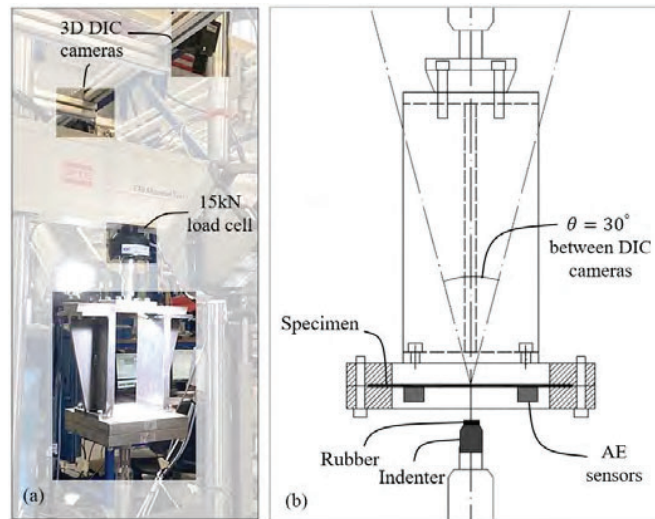

Figure 2. a) Experiment setup, b) illustration of the test fixtures.

2.3. Test procedure

Before the fatigue tests, a series of quasi-static tests with the identical test setup were performed under displacement control [16]. The maximum fatigue load was designed to be 80% of the critical load for quasi-static delamination initiation, resulting in $P_{max} = 3000$ N.

The fatigue tests were performed under force control with a load ratio $R = P_{min}/P_{max} = 0.1$, and a loading frequency of 2 Hz. To monitor delamination growth, the fatigue tests were halted after a predetermined number of loading cycles, at which point an echo-pulse C-scan was conducted. As illustrated in Figure 3, the echo-pulse C-scan facilitates the examination of delamination depth based on the Time-of-flight (TOF) of the pulse signals. Measurements of a_{init}, a_{migra}, and A_{tot}, were conducted

ECCM21

02-05 July 2024
Nantes - France

Proceedings of the 21st European Conference on Composite Materials
Volume 8 - Special Sessions

651
1420

CONTENTS

after a predetermined number of cycles, ensuring an increment of delamination growth within a range of 0.5 ~ 2.0 mm. The tests were terminated when the propagation rate was close to zero.

After testing, the delaminated region was sectioned and opened for fractographic analysis under a Scanning Electron Microscope (SEM), focusing specifically on the gray area highlighted in Figure 3.
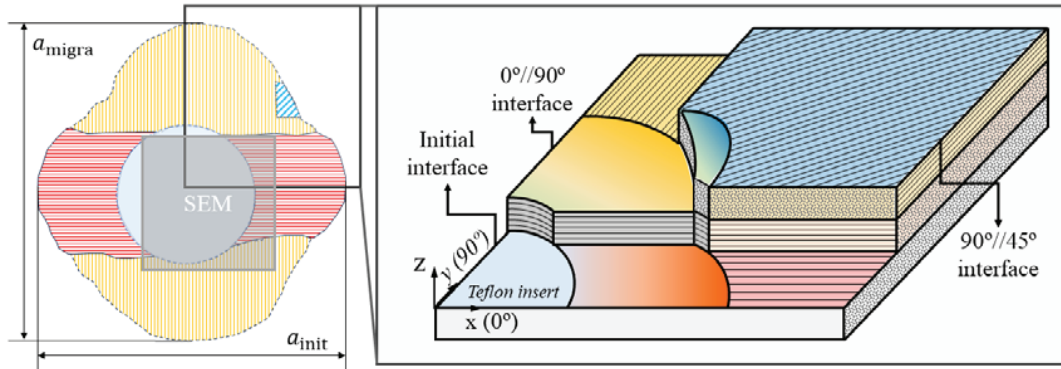

Figure 3. Planar fatigue delamination pattern of PCLS(0//0) depicted by C-scan. a_{init} and a_{migra} inidicate the maximum delamination length of initial interface and migration interface, respectively. The projected area of each C-scan image is measured as the total delamination area A_{tot}.
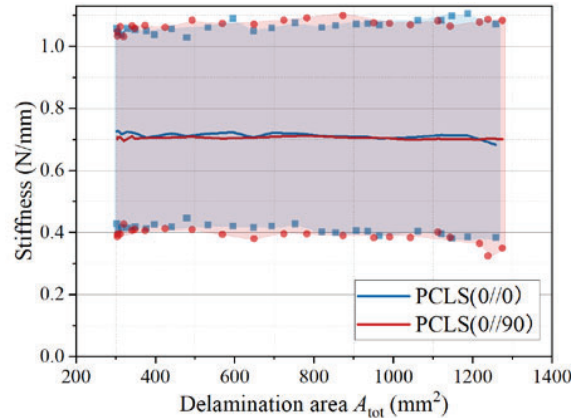
3. Results

3.1. Force-displacement response and stiffness variation

A representative force-displacement response of a series of cyclic loading and unloading processes is shown in Figure 4. Under force control, the hysteresis loop gradually shifted to the right, indicating a higher displacement level for sustaining the predefined load range. The energy loss in the hysteresis loop is mainly attributed to deformation of the rubber indenter tip, rather than delamination growth in a single cycle.
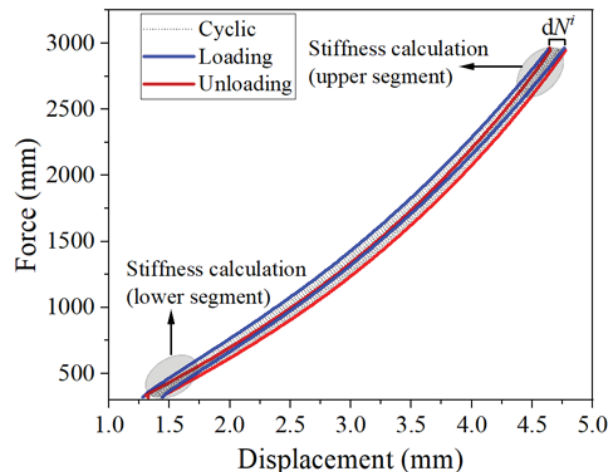
Figure 4. Cyclic force-displacement curves for calculation of cyclic energy dissipation.

The stiffness variation throughout the fatigue test was calculated by considering two segments in the force-displacement curves, corresponding to the lower and upper limits. As shown in Figure 5, the stiffness calculated from the upper segment is almost constant, while the lower segment presents a gradual decrease as the total delamination area increases. This indicates that fatigue delamination growth has a more pronounced effect on the the initial linear elastic behaviour than the geometric nonlinear behaviour associated with large deformation.

ECCM21

02-05 July 2024
Nantes - France

Proceedings of the 21st European Conference on Composite Materials
Volume 8 - Special Sessions

652
1420

Figure 5. Stiffness variation along the increasing fatigue delamination area. The scattered data points with higher and lower stiffness levels correspond to the stiffness cacluated at the upper and lower force-displacement segments. The solid curves represent the average stiffness.

3.2. Delamination growth

As shown in Figure 6, the measurement of delamination growth is performed by extracting delamination length at the initial interface (red region, a_{init}), migration interface (orange region, a_{migra}), and the total area of delaminated region A_{tot}. The propagation trend of three measurements were closely aligned for two different specimen configurations. Delamination migration occurred at an early stage of delamination growth. A rapid extension of the delamination area is presented within the first 10 000 cycles at both initial and migrated interfaces.

(a)

(b)
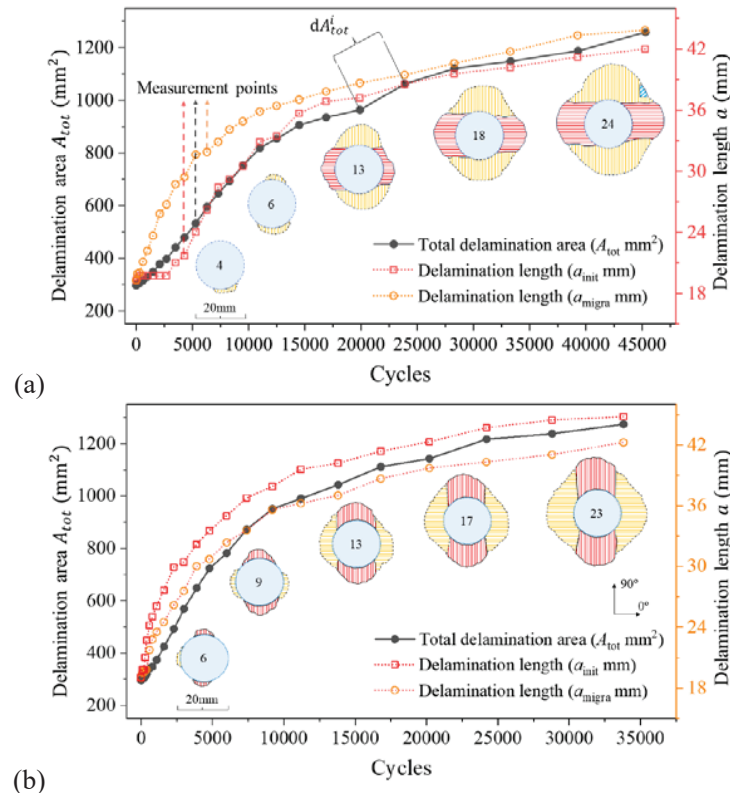
Figure 6. C-scan measurement of fatigue delamination growth of a) PCLS(0//0) and b) PCLS(0//90) specimens. The number in the C-scan images indicates the number of measurement points in the propagation curves.

ECCM21
02-05 July 2024
Nantes - France

Proceedings of the 21st European Conference on Composite Materials
Volume 8 - Special Sessions

653
1420

CONTENTS

For PCLS(0//0), a delayed initation of delamination growth at the initial 0º//0º interface is observed. This causes a smaller maximum delamination length at the initial interface compared to the migration interface. For PCLS(0//90), the angles between the initial and migration interfaces were identical, both were (0º//90º). Delamination growth at the initial interface is larger than that of the migration interface, regarding the maximum delamination length.

The variation of propagation rate, expressed as total increment of delamination area per cycle dA_{tot}/dN, is shown in Figure 7. Three stages can be recognized in the fatigue delamination process. At the beginning, an acceleration in the propagation rate is presented. Such rapid increase in the propagation rate is more obvious in the PCLS(0//90) specimen without delayed initation of delamination growth. Then, a decrease in the propagation rate is presented at phase II. At phase III, the propagation rate remains consistently low.

A similar propagation trend was observed in the 2D debonding test under force-controled fatigue loading [14]. This indicates that in the 2D fatigue test with force control and constant amplitude, a larger delamination area correlates with increased resistance to fatigue.
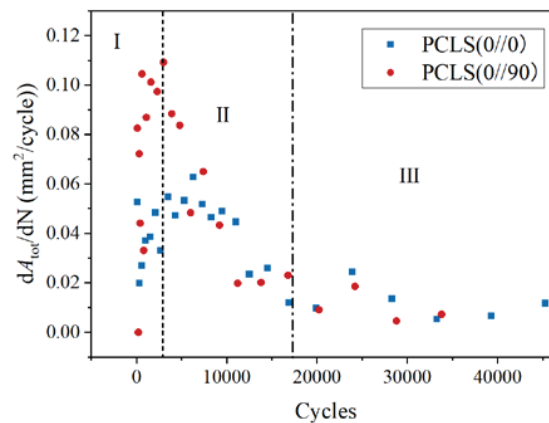

Figure 7. Variation of delamination growth rate.

3.3. Fractography and fatigue delamination mechanisms
In order to investigate 2D fatigue delamination mechanisms, fractographic observations were performed using SEM. As shown in Figure 8, several locations in the vicinity of the initial delamination front were selected for high-magnification SEM observations.
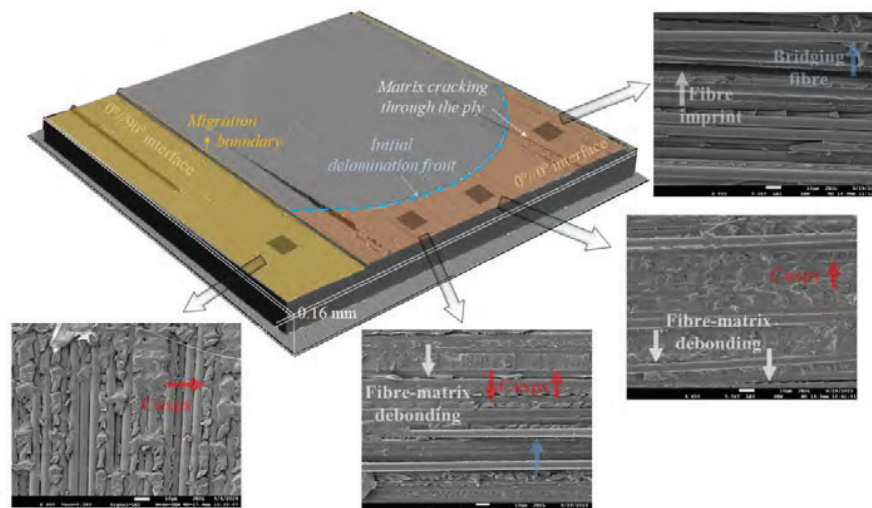

Figure 8. Fractographic observation at the delamination surface of PCLS(0//0).

ECCM21

02-05 July 2024
Nantes - France

Proceedings of the 21st European Conference on Composite Materials
Volume 8 - Special Sessions

654
1420

CONTENTS

Discrepancies in the fracture mechanisms were recognized at different locations. For delamination growth at the initial interface, matrix cracking and fibre-matrix debonding are dominant damage modes that facilitate delamination growth. As the misalignment between the fibre direction and the normal direction of the circular delamination front increases, more severe fibre-matrix debonding and through-thickness matrix cracking are exhibited. Such damage pattern triggers fibre bridging and delamination migration as the misalignment increases.

The delamination growth at the migration interface initiates from the migration boundary, and continues to propagate following the fibre orientation of an adjacent ply. The migrated delamination growth presents more shear-induced matrix cracks (cusps) compared to the delamination growth at the initial interface. The diverse fatigue fracture mechanisms across various locations contribute to the emergence of the observed delamination pattern.

4. Conclusions

An experimental method was proposed in this study to investigate planar delamination behaviour under cyclic out-of-plane indentation. An accurate measurement of delamination growth was achieved by using echo-pulse C-scan with TOF plotting. By analyzing the variations in the delamination growth rate, segmental stiffness, and fatigue fracture mechanisms, the following conclusions are drawn:

The interface fibre angles significantly influence the initiation of an embedded delamination, but have a minor effect on the delamination propagation pattern.

Despite slight differences in the delamination lengths at the initial and migrated interfaces, the growth rate trends at these interfaces are aligned. Three stages are presented in the delamination growth rate: a rapid initial increase at phase I, a gradual decrease in the growth rate at phase II, and a stable low growth rate at phase III.

The propagation of planar delamination had negligible effects on the overall stiffness of the specimens but had a considerable effect on their initial linear elasticity.

Planar delamination growth at different locations along the circular front was dominated by distinct fatigue fracture mechanisms. Shear induced matrix cracking, fibre-matrix debonding, and fibre pullout are the most recognizable mechanisms that facilitated delamination growth. As the misalignment between the principal growth direction and fiber direction increases, delamination migration can be triggered by through-thickness matrix cracking.

Given the strong correlation between growth curves extracted from delamination length and area, the Paris-type equation appears suitable for predicting planar delamination growth, contingent upon determining fracture parameters from the critical interface. Further research is needed to compare parameters acquired from 1D and 2D tests with the same interface.

References

[1] ASTM D5528-01, "Standard test method for mode I interlaminar fracture toughness of unidirectional fiber-reinforced polymer matrix composites," Am. Stand. Test. Methods, vol. 03, pp. 1–12, 2014.

[2] ASTM D7905, "Standard test method for determination of the mode II interlaminar fracture toughness of unidirectional fiber-reinforced polymer matrix composites," ASTM, pp. 1–18, 2014.

ECCM21
02-05 July 2024
Nantes - France

Proceedings of the 21st European Conference on Composite Materials
Volume 8 - Special Sessions

655
1420

CONTENTS

[3] P. Paris and F. Erdogan, "A critical analysis of crack propagation laws," J. Fluids Eng. Trans. ASME, vol. 85, pp. 528–533, 1963.

[4] G. L. Roderick, R. a Everett, and J. H. Crews Jr., "Debonding Propagation in Composite Reinforced Metals Tech Rep NASA TM X-71948," 1974.

[5] C. G. Dávila, "From S-N to the Paris law with a new mixed-mode cohesive fatigue model for delamination in composites," Theor. Appl. Fract. Mech., vol. 106, 2019.

[6] L. Yao, Y. Sun, R. C. Alderliesten, R. Benedictus, and M. Zhao, "Fibre bridging effect on the Paris relation for mode I fatigue delamination growth in composites with consideration of interface configuration," Compos. Struct., vol. 159, pp. 471–478, 2017.

[7] L. E. Asp, A. Sjögren, and E. S. Greenhalgh, "Delamination Growth and Thresholds in a Carbon/Epoxy Composite under Fatigue Loading," J. Compos. Technol. Res., vol. 23, pp. 55–68, 2001.

[8] F. M. Monticeli, H. J. C. Voorwald, and M. O. H. Cioffi, "The influence of carbon-glass/epoxy hybrid composite under mode I fatigue loading: Hybrid fiber bridging zone model," Compos. Struct., vol. 286, p. 115274, 2022.

[9] S. Stelzer, A. J. Brunner, A. Argüelles, N. Murphy, G. M. Cano, and G. Pinter, "Mode I delamination fatigue crack growth in unidirectional fiber reinforced composites: Results from ESIS TC4 round-robins," Eng. Fract. Mech., vol. 116, pp. 92–107, 2014.

[10] M. Hojo, T. Ando, M. Tanaka, T. Adachi, S. Ochiai, and Y. Endo, "Modes I and II interlaminar fracture toughness and fatigue delamination of CF/epoxy laminates with self-same epoxy interleaf," Int. J. Fatigue, vol. 28, pp. 1154–1165, 2006.

[11] I. Maillet, L. Michel, F. Souric, and Y. Gourinat, "Mode II fatigue delamination growth characterization of a carbon/epoxy laminate at high frequency under vibration loading," Eng. Fract. Mech., vol. 149, pp. 298–312, 2015.

[12] Y. Gong, L. Zhao, J. Zhang, and N. Hu, "Crack closure in the fatigue delamination of composite multidirectional DCB laminates with large-scale fiber bridging," Compos. Struct., vol. 244, 2020.

[13] L. Yao, R. C. Alderliesten, M. Zhao, and R. Benedictus, "Discussion on the use of the strain energy release rate for fatigue delamination characterization," Compos. Part A Appl. Sci. Manuf., vol. 66, pp. 65–72, 2014.

[14] A. Cameselle-Molares, A. P. Vassilopoulos, and T. Keller, "Two-dimensional fatigue debonding in GFRP/balsa sandwich panels," Int. J. Fatigue, vol. 125, pp. 72–84, 2019.

[15] A. Cameselle-Molares, A. P. Vassilopoulos, and T. Keller, "Experimental investigation of two-dimensional delamination in GFRP laminates," Eng. Fract. Mech., vol. 203, pp. 152–171, 2018.

[16] W. Tu, J.-A. Pascoe, and R. Alderliesten, "Planar delamination behaviour of CFRP panels under quasi-static out-of-plane loading," Compos. Struct., vol. 118137, 2024.

[17] R. C. Alderliesten, A. J. Brunner, and J. A. Pascoe, "Cyclic fatigue fracture of composites: What has testing revealed about the physics of the processes so far?," Engineering Fracture Mechanics, vol. 203. pp. 186–196, 2018.

[18] L. Amaral, L. Yao, R. Alderliesten, and R. Benedictus, "The relation between the strain energy release in fatigue and quasi-static crack growth," Eng. Fract. Mech., vol. 145, pp. 86–97, 2015.

[19] J.-A. Pascoe, "Slow-growth damage tolerance for fatigue after impact in FRP composites: Why current research won't get us there," Theor. Appl. Fract. Mech., vol. 116, p. 103127, 2021.

[20] R. C. Alderliesten, "How proper similitude can improve our understanding of crack closure and plasticity in fatigue," Int. J. Fatigue, vol. 82, pp. 263–273, 2016.

[21] H. J. Den Ouden, "Investigating Planar Delamination Behavior in Carbon Fiber Reinforced Polymer Panels An evaluation of delamination criteria," Delft University of Technology, 2020.

[22] C. Wang, A. P. Vassilopoulos, and T. Keller, "Numerical investigation of two-dimensional Mode-II delamination in composite laminates," Compos. Part A Appl. Sci. Manuf., vol. 179, p. 108012, 2024.

[23] C. Wang, A. P. Vassilopoulos, and T. Keller, "Experimental investigation of two-dimensional Mode-II delamination in composite laminates," Compos. Part A Appl. Sci. Manuf., vol. 173, p. 107666, 2023.

[24] Delta-Tech Italy, "Technical Data Sheet - DT120 Versatile High Toughness Epoxy Matrix," 2015.